Analysis of an Array of Rectangular Apertures Based on the Active Parameters of Its Infinite Extension

Laurențiu Iustin BUZINCU, Lucian ANTON, Daniel DEPĂRĂȚEANU, and Mircea NICOLAESCU

***Abstract*—The authors of the study under consideration employ the methods available in the literature in conjunction with the data obtained by modeling the active admittance of an element included in an infinite planar array of rectangular apertures, in order to draw conclusions regarding the operation of the elements of a finite array with the same geometry. The behavior of finite array's individual elements in relation with their positions within the array is investigated. Also, the global patterns of a bi-dimensional finite array and a monopulse array are calculated.**

***Index Terms*—planar array, infinite array, active admittance, active reflection coefficient, directivity pattern.**

I. Introduction

The authors of this paper employ the data generated by a previously-developed method for calculating element's active admittance of an infinite array of rectangular apertures in a ground plane by employing a mode-matching technique [6], in order to model the behavior of an arbitrary element included in a finite array under the influence of mutual coupling. The analysis is an adaptation based on an approach proposed by Roscoe [3].

II. Active Admittance and Coupling Admittances in an Infinite Array

The topology of the array considered in the following analysis, is given in Figure 1. The array has a rectangular $D_x \times D_y$ lattice and the numbering of the elements is also indicated in the figure. The geometrical parameters of the array are as follows: $D_x = 0.5715\lambda$, $D_y = 0.5355\lambda$, while the sizes of the rectangular apertures are $a = 0.4763\lambda$ and $b = 0.2333\lambda$. One should note that as the array extends to infinity, the position of the (*m,n*) element is arbitrary as it describes the position of each and every element of the infinite array. In the following, the dependence of the active admittance (understood as the input admittance of an arbitrary element of the infinite array) and the coupling parameters will be demonstrated.

This is an extended version of an article that was presented at Communications 2018, Bucharest, Romania.

L. I. Buzincu was with Military Technical Academy as a lecturer until 1998.

L. Anton is currently a conference professor at the Military Technical Academy, 39-49 George Coşbuc Ave., Sector 5, 050141, Bucharest, Romania, Bucharest, Romania.

D. Depărățeanu is an assistant professor at the Military Technical Academy, 39-49 George Coşbuc Ave., Sector 5, 050141, Bucharest, Romania Bucharest, Romania.

M. Nicolaescu is with Synopsys, Boston, USA.

Considering that $m = n = 0$, the following equation for the active admittance can be demonstrated:

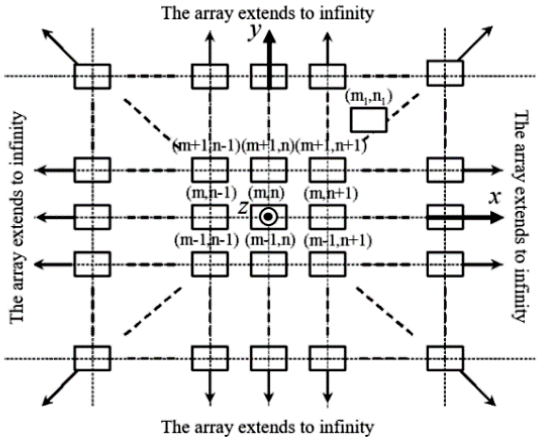

Figure 1. The topology of the infinite array. The elements are uniformly distributed in the (*x,y*) plane. The distances between the rows are D_x along the x axis and D_y along the y axis, respectively

$$Y_{ACT}(\xi,\mu) = \lim_{M\to\infty}\lim_{N\to\infty}\sum_{\nu=-M}^{M}\sum_{\eta=-N}^{N} y_{\nu,\eta} e^{j\nu\xi} e^{j\eta\mu} \tag{1}$$

The arguments of function $Y_{ACT}(\xi,\mu)$ can be written as:

$$\xi = kD_x \sin\theta\cos\varphi = kD_x u = \frac{2\pi D_x}{\lambda}u = \frac{2\pi u}{P_x} \tag{2}$$

$$\mu = kD_y \sin\theta\sin\varphi = kD_y v = \frac{2\pi D_y}{\lambda}v = \frac{2\pi v}{P_y} \tag{3}$$

$$P_x = \frac{\lambda}{D_x} \tag{4}$$

$$P_y = \frac{\lambda}{D_y} \tag{5}$$

In (1), the indices ν and η show that the position of the (ν,η) element relative to the element the active admittance of which is determined is given by the coordinates νD_x and ηD_y measured along the *x* and *y* axis respectively.

The quantities P_x and P_y indicate the fact that $Y_{ACT}(\xi,\mu)$ is periodic with respect to the variables (ξ,μ). Following a change of variables from (ξ,μ) to the direction cosines (u,v) the two-dimensional period in the (u,v) plane is marked in Figure 2 and is known as the "periodic rectangle".

Digital Object Identifier 10.32754/JMT.2018.1.03

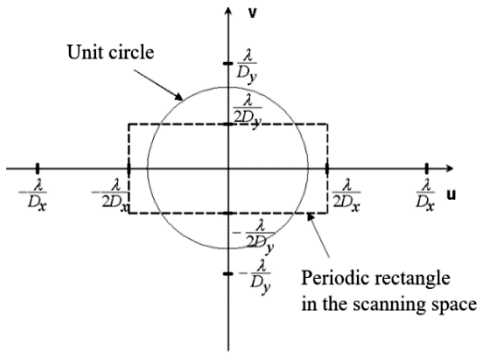

Figure 2. The (u,v) plane with the periodic rectangle and the unit circle marked

In Figure 2, the visible space (the values of the direction cosines corresponding to the half-space above the plane of the array) is also represented as the area inside the circle of unit radius in the (u,v) plane.

Taking into consideration the periodicity of function $Y_{ACT}(u,v)$, the coefficients of the function's Fourier Series decomposition are identified as the coupling admittances:

$$y_{v,\mu}=\frac{1}{P_x}\int_{-\frac{P_x}{2}}^{\frac{P_x}{2}}\frac{1}{P_y}\int_{-\frac{P_y}{2}}^{\frac{P_y}{2}}Y_{ACT}(u,v)e^{-jv\frac{2\pi}{P_x}u}e^{-j\mu\frac{2\pi}{P_y}v}dudv \tag{6}$$

The discrete values of the coupling admittances up to $\frac{N}{2}$ elements away, can be assessed by applying a Fast Fourier Transform (FFT) to the sampled values of the active admittance over the periodic rectangle as given in (7), (8) and (9)

$$u_p=\frac{p}{N}P_x=\frac{p\lambda}{ND_x}\quad p=-\frac{N}{2},-\frac{N}{2}+1,\ldots,\frac{N}{2}-1 \tag{7}$$

$$v_p=\frac{q}{N}P_y=\frac{q\lambda}{ND_y}\quad q=-\frac{N}{2},-\frac{N}{2}+1,\ldots,\frac{N}{2}-1 \tag{8}$$

$$\left[y_{p,q}\right]=\left(\frac{1}{N}\right)^2\mathrm{FFT2}\left[Y_{ACT}(u_p,v_q)\right] \tag{9}$$

III. Active Reflection Coefficient and the Directivity Function the Infinite Array Element

Based on the relation for active admittance, an active reflection coefficient can be defined as:

$$\Gamma(\xi,\mu)=\frac{Y_g^*-Y_{ACT}(\xi,\mu)}{Y_g+Y_{ACT}(\xi,\mu)} \tag{10}$$

From (1) to (6) it can be seen that the function $\Gamma(u,v)$ is also periodic over the (u,v) plane with the same periods P_x and P_y.

In order to find the directivity function of the element included in the infinite array, all the elements except for the one under analysis are terminated on the internal admittances of their generators (the generators are passivized). The directivity function of the element in the conditions previously specified is [4]:

$$f_e(u,v)=\frac{f(u,v)}{\sqrt{G_g}}\left[1+\Gamma(u,v)\right] \tag{11}$$

In (11), $f(u,v)$ is the directivity function of the isolated element which is demonstrated in [1] and [4], while G_g is the real part of generators' internal admittance. From (9) by dividing either side of the equation by $\frac{f(u,v)}{\sqrt{G_g}}$ one can note that the factor $[1+\Gamma(u,v)]$ is proportional to the directivity function of an infinite array of Huygens sources where the interactions between the elements of the array are the same as for the original array. A Fourier series decomposition of $[1+\Gamma(u,v)]$ will therefore provide the excitations induced to each and every element of the array of Huygens sources:

$$1+\Gamma(u,v)=\lim_{M\to\infty}\lim_{N\to\infty}\sum_{v=-\frac{M}{2}}^{\frac{M}{2}}\sum_{\eta=-\frac{N}{2}}^{\frac{N}{2}}S_{v,\eta}e^{jv\frac{2\pi}{T_x}}e^{j\eta\frac{2p}{T_y}} \tag{12}$$

$$S_{v,\mu}=\frac{1}{P_x}\int_{-\frac{T_x}{2}}^{\frac{T_x}{2}}\frac{1}{P_y}\int_{-\frac{T_y}{2}}^{\frac{T_y}{2}}Y_{ACT}(u,v)e^{-jv\frac{2\pi}{P_x}u}e^{-j\mu\frac{2\pi}{P_y}v}dudv \tag{13}$$

Reiterating the reasoning of the previous section, a FFT is applied in order to obtain the excitations mentioned above:

$$\left[S_{p,q}\right]=\left(\frac{1}{N}\right)^2\mathrm{FFT2}\left[1+\Gamma\left(u_p,v_q\right)\right] \tag{14}$$

IV. Finite Array Modelling Based on the Infinite Array Parameters

The first step in modeling the array was to obtain the values of the coupling admittances as indicated in (9). The active admittance was sampled on a 64 by 64 grid over the periodic rectangle. An E-plane cut (along the *y* axis) of the results is given in Figure 3.

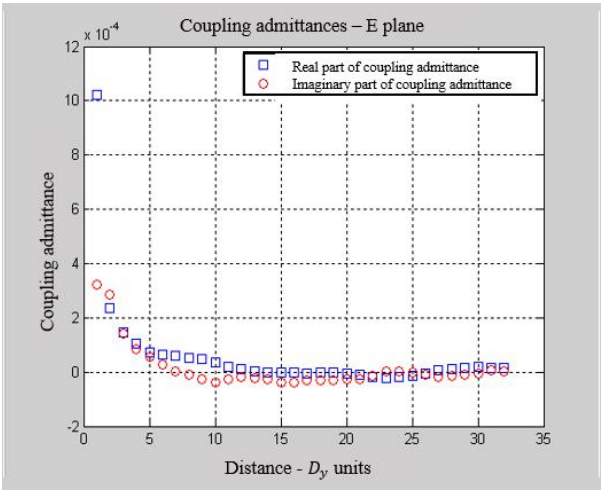

Figure 3. E plane cut (*y* axis) values of the real and imaginary values of the coupling admittances

In order to check out the consistency of the calculation, the following computer experiment was conducted: the active admittance of an array with doubled lattice size $2D_x \times 2D_y$ was calculated and sampled over a 32 by 32 grid over the periodic rectangle and the coupling admittances were extracted by the same procedure. The values were compared with those obtained for the original array and a good consistency was demonstrated, as illustrated in Figure 4.

The second step was to truncate the infinite array to a finite one. In order to achieve that, the physical processes involved in the operation of the apertures in a ground plane were considered. As far as the admittance parameters were concerned, shunting the excess elements in order to obtain an arbitrary finite array of rectangular apertures in a ground plane appeared as a sound working hypothesis. Definitely, by short-circuiting the excess elements, the electric fields in the apertures would be nullified and thus, their contribution to the total radiated field cancelled. On the other hand, in the case of the excitations calculated by (14) the truncation consisted in simply ignoring the excitations of the excess elements.

This approach is less intuitive than the former truncation but, as will be shown, still provides valuable information regarding the operation of the array.

On the other hand, in the case of the excitations calculated by (14) the truncation consisted in simply ignoring the excitations of the excess elements which is less intuitive than the former truncation but, as will be shown, still provides valuable information regarding the operation of the array.

The modeling presented henceforth, consisted in simulating the operation of the center, E plane and H plane boundary elements and upper right corner elements of a rectangular array of 21 by 21 elements, obtained by truncating the infinite array as detailed above. The actual positions of the elements are described within the figures.

By obtaining the coupling admittances in (9), an admittance matrix of the finite array could be assembled. From the admittance matrix, the scattering matrix of the finite array was calculated. As far as the excitation is concerned, only the elements of interest, as indicated above, were provided with input power.

The rest of the excitations are the results of the mutual coupling among the elements of the array as all but one, have their generators rendered passive.

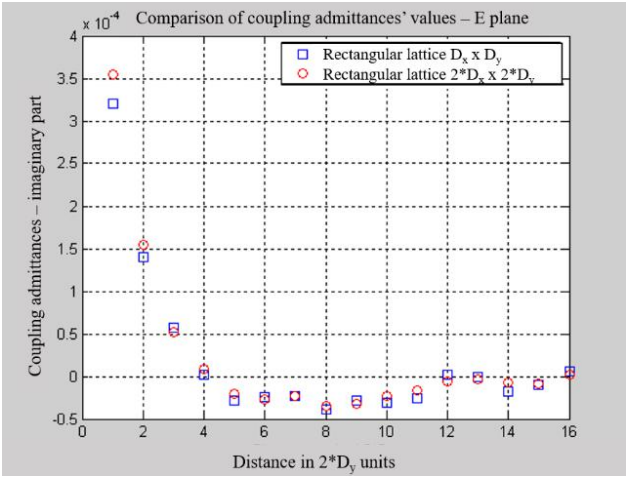

Figure 4. An E plane cut (*y* axis) comparison between the values of the coupling admittances of the original array and one with a double-size lattice

The general equations for the calculation of overall array excitations are given by (15) and (16):

$$\mathbf{b} = \mathbf{Sa} \tag{15}$$

$$\mathbf{EXCITATIONS} = \mathbf{a} + \mathbf{b} \tag{16}$$

where **b** is the vector of reflected waves, **a** is the vector of direct waves and **S** is the scattering matrix.

The excitations thus determined were introduced in a MATHLAB program designed to compute the directivity function of the array of Huygens sources with arbitrary excitations and afterward the results were multiplied to the corresponding values from the isolated element. This approach was adapted from the Method of Coupling Admittances (CA) as defined in [3].

Similarly, the output from (14), where an assessment of the excitations was provided directly, was processed after the corresponding truncation, in a manner identical to the excitations resulting from (16). This approach is a simplified version of the Method of Direct Fourier Window (DFW) as defined in [3].

The left side of (11) allows for the assessment of the directivity pattern of the element included in the infinite array.

The directivity patterns in Figures 5 and 6 are the results calculated for the central element (the position of the element is shown in both figures) of a 21 by 21 array by employing MATHLAB codes based on the methods detailed above. On the same diagrams, the pattern of a standalone element and also that of the element included in the infinite array are also represented. It is significant to note that even though, the patterns of the elements included in arrays are significantly different from those of the standalone element, the similarity among them is obvious. The patterns calculated by employing CA and DFW are essentially identical on the other hand, DFW is easier to implement.

Therefore, it can be concluded that DFW is a useful tool that can be employed for a first evaluation of elements' behavior.

In addition, there are no significant differences between the pattern of the element of the infinite array and the pattern of the central element of the finite array which recommends a practical, experimental method for assessing the accuracy of the theoretical models.

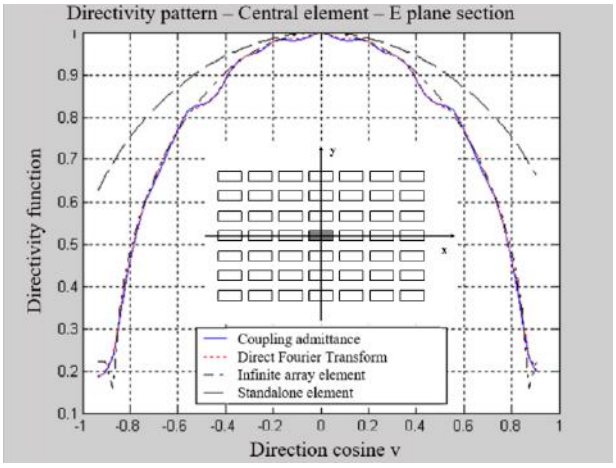

Figure 5. 21 by 21 planar finite array central element directivity pattern – E plane cut, calculated by the methods of Coupling Admittances and Direct Fourier Window

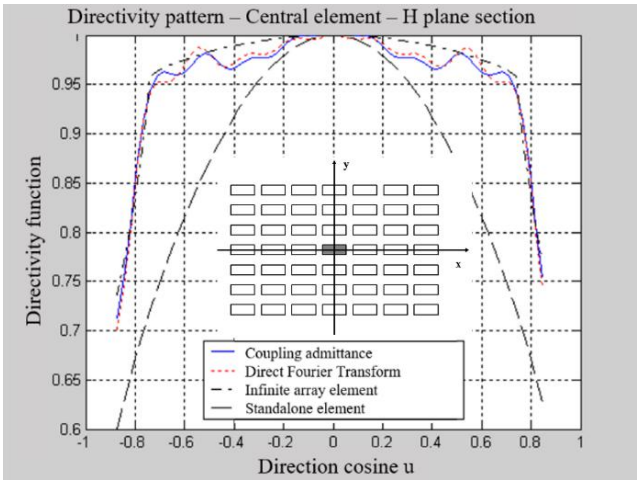

Figure 6. 21 by 21 planar finite array central element directivity pattern – H plane cut, calculated by the methods of Coupling Admittances and Direct Fourier Window

In the following, additional simulations are given in order to show the behavior of elements removed from the center of the array.

In the beginning, the pattern of an element situated in the middle of the top boundary of the array (Figure 7) was calculated.

As can be noted, the pattern is significantly distorted in the E-plane when compared with the pattern of the central element which will be used, from here on, as a measure of the effects of coupling on the behavior of the rest of the elements taken into consideration.

The next situation which was taken into consideration was that of an element situated in the middle of the right edge of the array, as shown in Figure 8.

As expected, the pattern is distorted in the H-plane, a result in good agreement with the previous simulation. The analysis was completed by calculating the patterns of a corner element.

In Figures 9 and 10, the results obtained for the corner element (as it is identified within the figures) are provided. As expected, the eccentric position of the element produced a significant distortion in element's directivity pattern which became asymmetrical in both E and H planes.

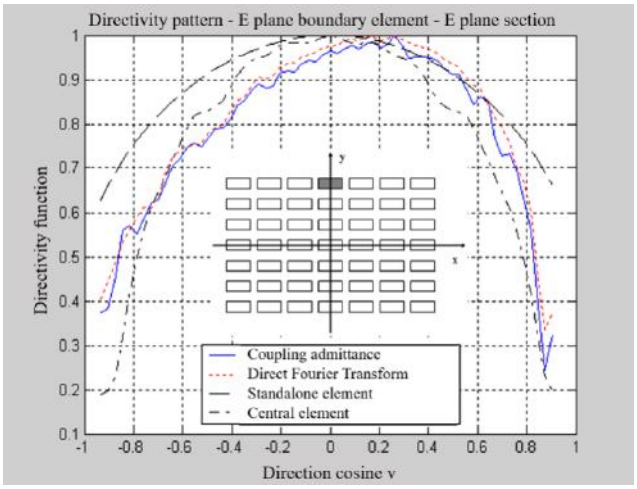

Figure 7. 21 by 21 planar finite array E plane boundary element directivity pattern – E plane cut, calculated by the methods of Coupling Admittances and Direct Fourier Window

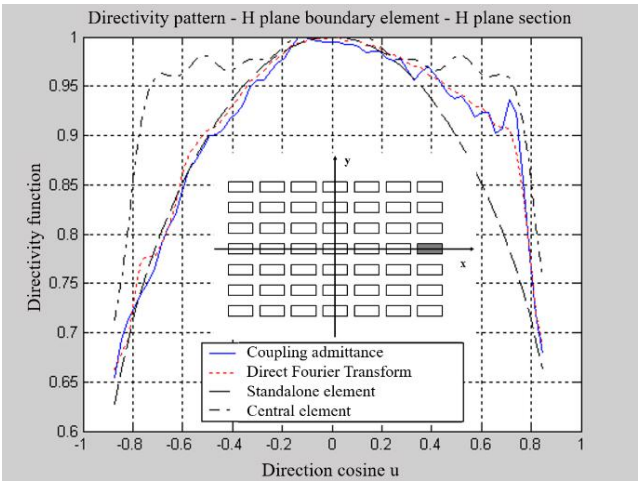

Figure 8. 21 by 21 planar finite array H plane boundary element directivity pattern – H plane cut, calculated by the methods of Coupling Admittances and Direct Fourier Window

There is excellent agreement among the results obtained in the previous two simulations and those generated for the corner element.

It can be inferred that, in the case of this particular topology of the array, the more stand-off from the central element and the more eccentric the assessed element is, the more significant the distortion of element's pattern will be.

The mentioned effect on the directivity pattern of the element could be proven important while employing the array for an application involving array signal-processing, because the behavior of the elements included in the array will not be uniform. Due to mutual coupling, the signals received by the individual sensors included in the array will be correlated and therefore, a basic prerequisite involved in the development of most signal processing algorithms will not be met. Nevertheless, the results obtained in the simulations above show the effects of mutual coupling among the elements can be assessed and employed in order to provide a better modeling of the real array. A possible development of the present analysis could be that of including in the model possible hardware solutions intended to cancel or to mitigate for the effects of mutual coupling.

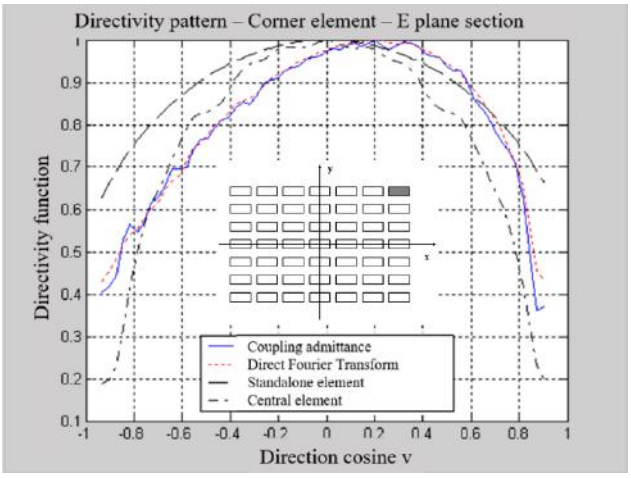

Figure 9. 21 by 21 planar finite array corner element directivity pattern – E plane cut, calculated by the methods of Coupling Admittances and Direct Fourier Window

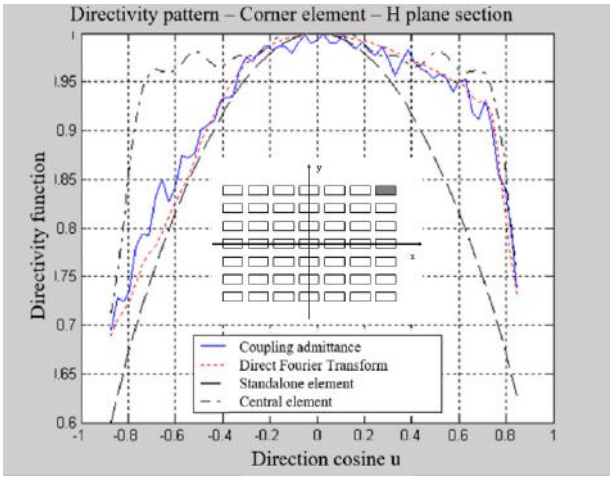

Figure 10. 21 by 21 planar finite array corner element directivity pattern – E plane cut, calculated by the methods of Coupling Admittances and Direct Fourier Window

It can be mentioned that the results obtained here are qualitatively similar with those presented by Roscoe [3].

The potential utility of the results presented here is demonstrated by employing the CA method for calculating the patterns of a finite (7×7) bi-dimensional array with a uniform excitation. The results are shown in Figure 11. The results were compared to the pattern of a coupling-free, ideal array. One can note that while within the mainlobes the patterns are virtually identical, the positions of the local maxima corresponding to the sidelobes do not overlap. In addition, while the pattern of the ideal array has clearly identifiable nulls, the pattern of the array with coupled elements shows finite minima.

The modelling was completed by introducing a linear phase-shift among the elements of the array in order to steer the beam. With the view to comparing the results from the in-phase array and the steered array, a 33.37 degrees E-plane steering was simulated. The results are given in Figure 12. It can be noted that, similar to the situation of in-phase excitation, the effects of steering are more easily identifiable outside the angular sector occupied by the main beam. Indeed, the positions of the sidelobes do not overlap and there are no nulls in the pattern of the array with coupling.

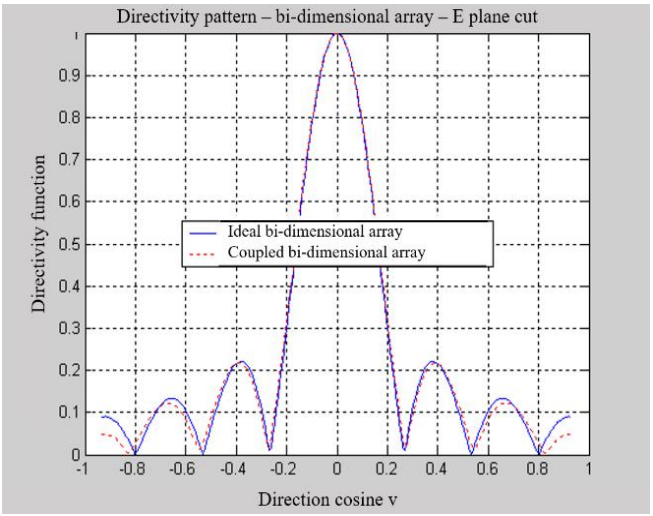

Figure 11. 7 by 7 in-phase planar finite array directivity pattern – E plane cut

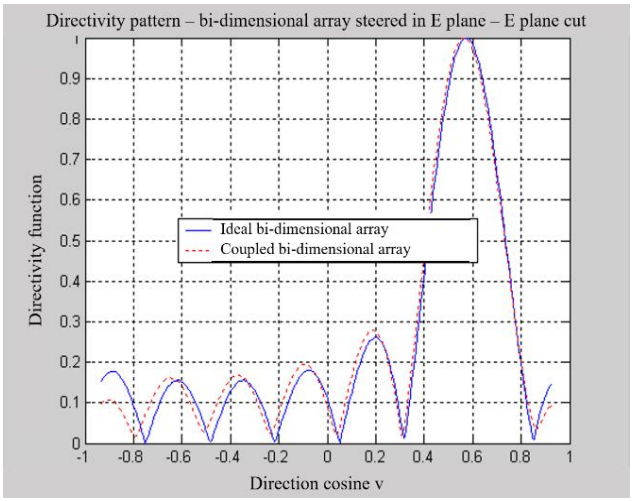

Figure 12. 7 by 7 planar finite array E plane steered directivity pattern – E plane cut

Finally, the behavior of a 8×8 monopulse array was investigated. The excitation of the array was such as an E-plane monopulse pattern was generated. Again, the results were compared with the pattern of an ideal array where the effects of mutual coupling were ignored. In the case of the in-phase excitation (monopulse array without steering), the pattern in Figure 13 shows that the position of the central nulls of the two patterns overlap. In addition, the shapes of the patterns within the angular sector where the array is supposed to provide angular discrimination are the same and therefore, in this particular situation, the coupling has no influence on the performance of the monopulse antenna array. Conversely, when the monopulse array was steered in the E-plane to an angle identical to the previous computer experiment (Figure 14), a deviation from the ideal case was found both in the position of the central null and also in the shape of the discriminator directivity pattern. Thus, one can conclude that depending of the elements and the topology of the array, mutual coupling can produce distortions in the monopulse pattern of the array and therefore errors in the discrimination of targets. Therefore, solutions are required to mitigate for the effects of mutual coupling in monopulse steered arrays.

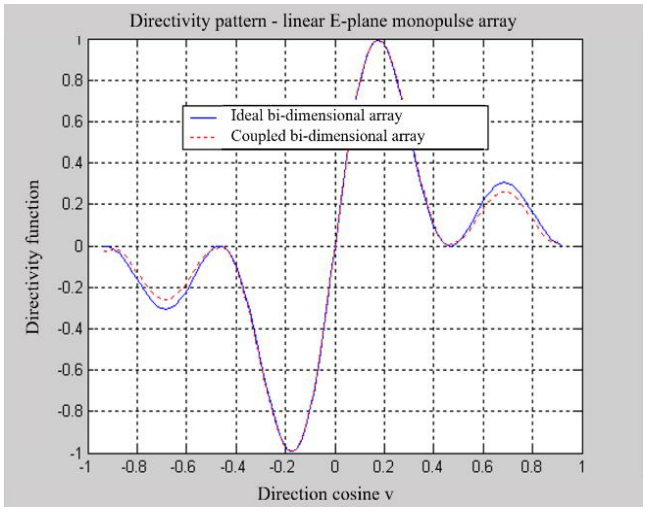

Figure 13. Pattern of an 8×8 E-plane monopulse array. The case of in-phase excitation

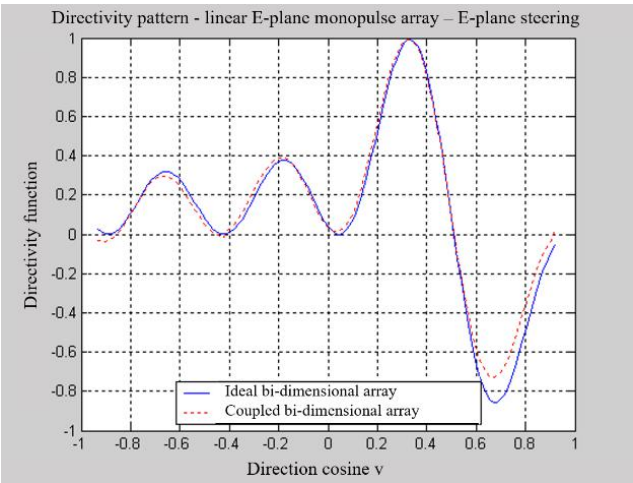

Figure 14. Pattern of a steered 8×8 E-plane monopulse array

V. CONCLUSION

The analysis presented in this paper demonstrated that there is practical utility in taking into consideration mutual coupling among the elements, while developing applications involving finite antenna arrays such as radar or communications scanning and signal processing antennas. The behavior of the elements of the array as a result of mutual coupling was demonstrated by conducting computer experiments based on the parameters previously calculated for arrays with identical topologies but extended to infinity [6]. Thus, a direct relationship between the parameters of the finite array and those of its infinite extension that can be modeled by employing a relatively simple mathematical apparatus, was demonstrated. As a general conclusion, it is obvious that mutual coupling has to be taken into consideration whenever the mathematical model of the application under scrutiny supposes that the elements of the array operate independently in other words, spurious correlation amongst the signals received by different coupled sensors might require the reassessment of the original algorithms and additional processing in order to compensate for it.

REFERENCES

[1] R. F. Harrington, *Time-Harmonic Electromagnetic Fields*, New York McGraw-Hill Book Comp., 1961.

[2] D. F. Kelley, W. L. Stutzman, "Array Antenna Pattern Modeling Methods that Include Mutual Coupling Effects," *IEEE Trans. on Antennas and Propagation*, vol. 41, no. 12, pp. 1625-1632, Dec., 1993. doi: 10.1109/8.273305

[3] A. J. Roscoe, R. A. Perrott, "Large Finite Array Analysis Using Infinite Array Data," *IEEE Trans. on Antennas and Propagation*, vol. 42, no. 7, pp. 983-992, Jul., 1994. doi: 10.1109/8.299601

[4] S. Silver, *Microwave Antenna Theory and Design*, New York, McGraw-Hill, 1953.

[5] L. I. Buzincu, "Contributions to Mutual Coupling Effect Analysis in Antenna Phased Arrays," PhD dissertation, Electronics and Telecommunications, Military Technical Academy, Bucharest, Romania, 2003.

[6] L. I. Buzincu, "A Method for the Analysis of an Infinite Array of Apertures in a Ground Plane," *MTA Review*, vol. XXVII, no. 2, pp. 99-104, Dec., 2017.